# An Investigation of Austenitic Stainless Steel Hot Rolled Angle Sections under Axial Compression

***Arthur A. de Menezes[a], Pedro C. G. da S. Vellasco[b], Luciano R. O. de Lima[b] and André T. da Silva[b]***

*Civil Engineering Post Graduate Program, State University of Rio de Janeiro – UERJ, Brazil[(a)]*
*Structural Engineering Department, State University of Rio de Janeiro – UERJ, Brazil[(b)]*

## Abstract

The flexural and the flexural-torsional buckling are stability phenomena and the controlling limit state for carbon steel angle columns. When austenitic stainless steel elements are considered some structural response differences are expected and motivated the present investigation. One of its aims was to enlarge the available experimental data for austenitic angles under compression. To fulfil these objectives, thirteen specimens were tested on 64x64x6.35 hot rolled angles with lengths varying from 250 mm to 1500 mm. These results were finally compared to the Eurocode 3 pt. 1-4 and to the Continuous Strength Method design provisions.

## Keywords

Stainless steel, Torsional buckling, Columns, Angles, Steel design.

## 1 Introduction

With the growing desire to reduce the impacts on the environment and the adoption of sustainable practices, the building construction methods were completely reshaped by applying new architectures, materials and technologies. The stainless steel has a role directly connected to these practices due to high resistance to corrosion. However, its cost interferes directly impacting its adoption in construction. One of the main causes of this derives from the way in which the manuals and regulatory institutes address their design since a vast number of stainless steel design standards are still based on carbon steel design concepts that are very conservative for the stainless steel.

Among the main existing international stainless steel design standards, the Eurocode 3 Part 1-4[1] is one of the most frequently updated, but there is still a wide range of concepts and parameters to be confirmed and validated. Some additional improvements to the stainless steel structural design conduct to the Continuous Strength Method (CSM) proposed by Ashraf and Gardner[2] centred on the development of criteria for a more efficient design of stainless steel structural elements. Within this perspective, the number of investigations related to the response of stainless steel compressed elements is still scarce and when hot rolled sections are considered this number is even lower and served as motivation for this investigation. The performed tests adopted a cross section made of angles, which has its geometry shown in Figure 1.

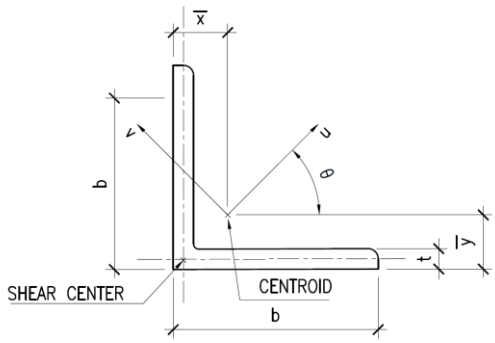


**Fig. 1 Angle section geometric properties**

## 2 Background and Stainless Steel Design Standards

One of the characteristics that the stainless steel differs from carbon steel is the stress *versus* strain curve that presents a nonlinear behaviour from the beginning, without a yield plateau. Stainless steels are an anisotropic material only presenting a constant elasticity modulus at low strain levels featuring higher tensile rupture stresses and higher ductility. Alternatively, the residual stresses resulting from the manufacturing process bars tend to be larger.

Stainless steel studies within structural engineering aim to adapt the design methods to the actual characteristics of stainless steel since analogies with carbon steel largely employed in international design standards lead to conservative structural solutions.

## 2.1 Eurocode 3 Part 1-4 [1]

According to the European design standard Eurocode 3 Part 1-4[1], the local buckling of angles subjected to compression must initially consider the cross-section class, Figure 2. The classes to these ultimate limit states are:

- class 3: the cross-section is able for reaching the yield stress before the local buckling onset;
- class 4: the cross-section is not able for reaching the yield stress leading to a reduction of its capacity in line with the loss of resistance associated with the elastic local buckling occurrence.

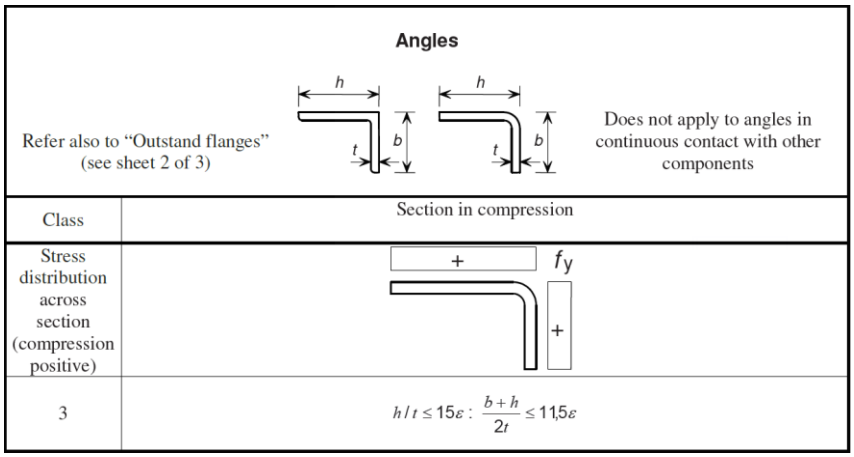


**Fig. 2 Width/Thickness ratio limit forsection classification [1]**

If the section belongs to class 4, the slender elements cross section area adopted in the compression design must be reduced according to the following equations:

$$\rho = \frac{1}{\bar{\lambda}_p} - \frac{0.188}{\bar{\lambda}_p^2} \leq 1.0 \tag{1}$$

$$\bar{\lambda}_p = \frac{(\bar{b}/t)}{28.4\varepsilon\sqrt{k_\sigma}} \tag{2}$$

where: $\rho$ is the element cross-section area reduction factor; $\lambda_p$ is the normalised slenderness; $b$ is the angle leg width; $t$ is the angle thickness; $\varepsilon$ is the material classification factor used to classify the section elements; $k_\sigma$ is the buckling coefficient equal to 0.43 for the angle legs.

The Eurocode 3 Part 1-4[1] recommends that the buckling global resistance of a structural element subjected to compression must be evaluated by equations (3) and (4):

$$N_{Rd} = \frac{\chi A f_y}{\gamma_{M1}} \quad \text{for Class 1 to 3 sections} \tag{3}$$

$$N_{Rd} = \frac{\chi A_{eff} f_y}{\gamma_{M1}} \quad \text{for Class 4 sections} \tag{4}$$

The column reduction factor $\chi$ considers factors such as the initial column imperfections, residual stresses levels, among others. Figure 3 depicts the variation of this reduction factor as the normalised slenderness for each column type or phenomenon while equations (5) to (10) illustrate how this parameter must be evaluated.

$$\chi = \frac{1}{\phi + \left[\phi^2 - \bar{\lambda}^2\right]^{0,5}} \tag{5}$$

$$\phi = 0.5\left(1 + \alpha\left(\bar{\lambda} - \bar{\lambda}_0\right) + \bar{\lambda}^2\right) \tag{6}$$

$$\bar{\lambda} = \sqrt{\frac{A_g f_y}{N_{Cr}}} \quad \text{for Class 1 to 3 sections} \tag{7}$$

$$\bar{\lambda} = \sqrt{\frac{A_{eff} f_y}{N_{Cr}}} \quad \text{for Class 4 sections} \tag{8}$$

$$N_{Cr} = \frac{\pi^2 EI}{(kL)^2} \quad \text{for flexural buckling} \tag{9}$$

$$N_{Cr} = \frac{1}{i_0^2}\left(GI_T + \frac{\pi^2 EI_w}{(kL)^2}\right) \quad \text{for torsional buckling} \tag{10}$$

The Eurocode 3 Part 1-4 [1] does not establish any specific criteria for hot rolled profiles, as can be observed in Table 1. In the comparison here performed the $\alpha = 0.49$ and $\lambda_0 = 0.40$ parameters adopted the values indicated for flexural buckling of open cold formed steel sections to evaluate the column reduction factor $\chi$.

**Table 1 Values of $\alpha$ and $\lambda_0$ for flexural, torsional and torsional-flexural buckling [1]**

| Buckling mode | Type of member | $\alpha$ | $\overline{\lambda_0}$ |
|---|---|---|---|
| Flexural | Cold formed open sections | 0.49 | 0.40 |
| | Hollow sections (welded and seamless) | 0.49 | 0.40 |
| | Welded open sections (major axis) | 0.49 | 0.20 |
| | Welded open sections (minor axis) | 0.76 | 0.20 |
| Torsional e Flexural-torsional | All members | 0.34 | 0.20 |

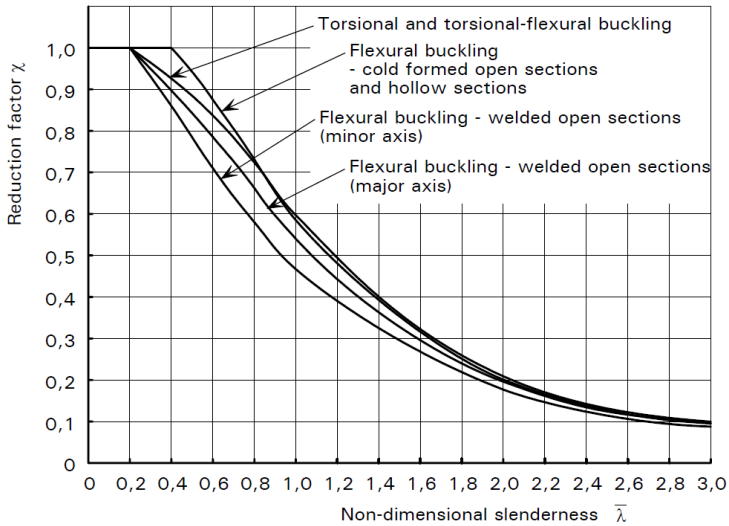


**Fig. 3 Buckling curves associated to flexural, torsional and flexural-torsional buckling [3]**

## 2.2 Continuous Strength Method - CSM [2]

The authors of this method proved that compact stainless steel sections have their load carrying compression strengths conservatively evaluated by Eurocode 3 Part 1-4 [1]. The main reason for this affirmative is that the Eurocode 3 Part 1-4 is based on criteria parameters similar to those of carbon steel. Figure 4 shows the results obtained in experiments with short columns and the prediction of their ultimate loads by Eurocode 3 Part 1-4 [1]. The results are presented regarding the cross-section elements slenderness, indicating that, for profiles with low slenderness, their ultimate loads can be underestimated by up to 50% [2].

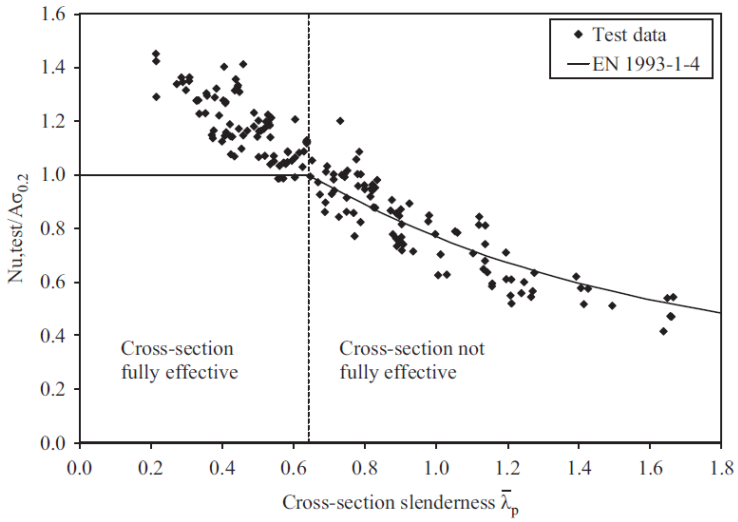


**Fig. 4 Comparison of 81 stub column test results with EN1993-1-4 provisions [2]**

In this design method, the slenderness of the elements is calculated from equation (2), as in Eurocode 3 Part 1-4[1]. For sections with slenderness $\lambda_p \leq 0.68$, the material reaches stresses values higher than the ones corresponding to deformation of 0.2% due to their nonlinear behaviour, as can be seen in Figures 4 and 5.

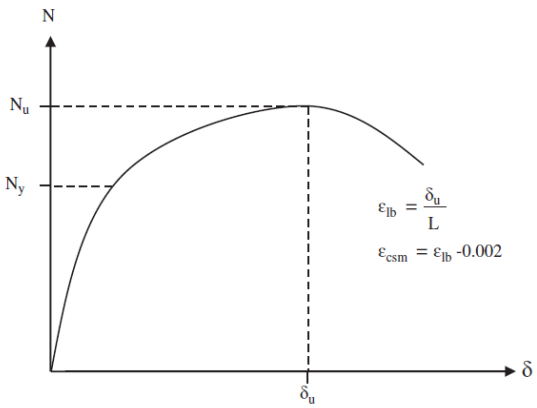


**Fig. 5 – Stub column load end-shortening response ($N_u > N_y$) [2]**

For cross sections with slenderness $\lambda_p \leq 0.68$ :

$$\frac{\varepsilon_{csm}}{\varepsilon_y} = \frac{\varepsilon_{lb} - 0.002}{\varepsilon_y} = \frac{\delta_u/L - 0.002}{\varepsilon_y} \quad \text{for } N_u \geq N_y \tag{11}$$

$$\frac{\varepsilon_{csm}}{\varepsilon_y} = \frac{N_u}{N_y} \quad \text{for } N_u < N_y \tag{12}$$

where: $N_u$ is the column load carrying capacity; $N_y$ is the section yield load corresponding to a 0.2% strain; $\delta_u$ is the column axial displacement; $L$ is the column length; $\varepsilon_{CSM}$ is the local buckling strain proposed by the method; $\varepsilon_y$ is the strain corresponding to the yield stress.

For section slenderness $\lambda_p > 0{,}68$ , leads to:

$$\frac{\varepsilon_{csm}}{\varepsilon_y} = \frac{N_u}{N_y} \tag{13}$$

Correlating the stainless steel behaviour with equations 11 to 13; the section deformation capacity can be evaluated with:

$$\frac{\varepsilon_{csm}}{\varepsilon_y} = \frac{0.25}{\bar{\lambda}_p^{3.6}} \quad \text{but} \quad \frac{\varepsilon_{csm}}{\varepsilon_y} \leq \min\left(15, \frac{\varepsilon_u}{\varepsilon_y}\right) \tag{14}$$

The material is characterised by a simple bilinear function. When the stress *versus* strain curve reaches the 0.2% stress, the initial Young's modulus E is established. From this point onwards this module decreases to $E_{sh}$, to represent the material strain hardening until the deformation limit of 0.16 $\varepsilon$, when it reaches the material ultimate tensile rupture stress. These variables can be calculated using the equations (15) and (16). Figure 6 shows a comparison of this model and the Ramberg-Osgood formulation.

$$\varepsilon_u = 1 - \frac{f_y}{f_u} \tag{15}$$

$$E_{sh} = \frac{f_u - f_y}{0.16\varepsilon_u - \varepsilon_y} \tag{16}$$

where: $E_{sh}$, is the stainless steel elasticity module, adopted in the CSM[2], $f_u$ is the material tensile rupture stress;

Assuming these criteria for compact sections the ultimate material stress is:

$$f_{csm} = f_y + E_{sh}\varepsilon_y\left(\frac{\varepsilon_{csm}}{\varepsilon_y} - 1\right) \tag{17}$$

where: $f_{csm}$ is the ultimate material stress adopted in CSM[2].

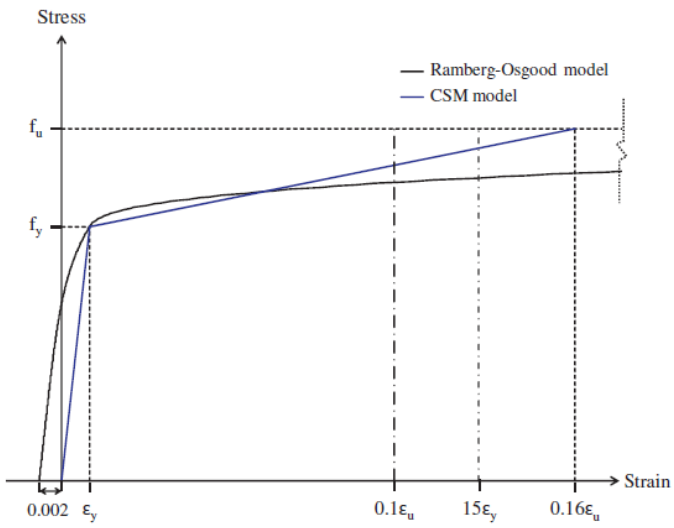


**Fig. 6 CSM elastic, linear hardening material model [2]**

# 3 Experimental Investigation

## 3.1 Tests Overview

For a better understanding of the structural behaviour of columns subjected to compression, thirteen tests were performed in the Civil Engineering Laboratory of the State University of Rio de Janeiro. The adopted cross-section was an L64x64x6.35 hot rolled angle made of austenitic stainless steel ASTM A276 304. Two of these tests were used for the material characterization measured through an actual compression test. Table 2 summarises the geometrical characteristics of the performed tests.

## 3.2 Test layout and support conditions

The tests aimed to reproduce situations of columns only subjected to compression to determine the maximum capacity of the angle section for each studied normalised slenderness. The tests were performed at a servo controlled Universal Lousenhausen test machine with a displacement control capacity suited for these tests. Figure 7 illustrates the test layout.

Various measurements were made to minimise the load application eccentricities such as: performing a cut perpendicular to the column axis; use of plates at the ends to even distribution of stresses in the contact between the press and the angle, leading to a greater accuracy of the results.

**Table 2 Test geometry**

| Test | Length (mm) | $b_1$ (mm) | $t_1$ (mm) | $b_2$ (mm) | $t_2$ (mm) |
|---|---|---|---|---|---|
| Characterization 1 | 250 | 64,00 | 6,50 | 64,00 | 6,54 |
| Characterization 2 | 250 | 64,30 | 6,48 | 64,00 | 6,34 |
| L64x64x6.4-AUS-500-1-23.09 | 488 | 63,63 | 6,40 | 63,56 | 6,48 |
| L64x64x6.4-AUS-500-2-23.09 | 491 | 63,95 | 6,42 | 63,76 | 6,32 |
| L64x64x6.4-AUS-750-1-27.09 | 738 | 63,68 | 6,60 | 63,78 | 6,43 |

| | | | | | |
|---|---|---|---|---|---|
| L64x64x6.4-AUS-750-2-28.09 | 736 | 63,75 | 6,57 | 63,67 | 6,34 |
| L64x64x6.4-AUS-1000-1-25.08 | 1000 | 63,72 | 6,42 | 63,42 | 6,65 |
| L64x64x6.4-AUS-1000-2-01.09 | 1000* | 63,60 | 6,55 | 63,73 | 6,35 |
| L64x64x6.4-AUS-1000-3-19.09 | 1000* | 63,65 | 6,52 | 63,78 | 6,36 |
| L64x64x6.4-AUS-1250-1-05.10 | 1238 | 63,53 | 6,52 | 63,75 | 6,29 |
| L64x64x6.4-AUS-1250-2-07.10 | 1241 | 63,55 | 6,47 | 63,78 | 6,34 |
| L64x64x6.4-AUS-1500-1-13.10 | 1491 | 63,70 | 6,44 | 63,82 | 6,50 |
| L64x64x6.4-AUS-1500-2-13.10 | 1492 | 63,69 | 6,37 | 63,78 | 6,42 |

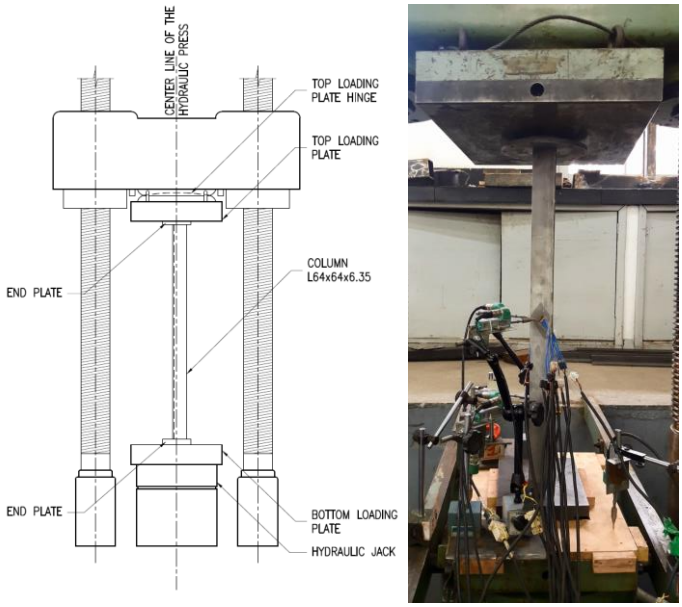


**Fig. 7 Tests layout**

## 3.3 Material Properties

Two compression tests made in 250 mm length short columns were performed to evaluate the adopted austenitic steel stress *versus* strain curve and their corresponding parameters. The main aim of these tests was to represent as accurately as possible the material response under compression in a direction parallel to rolling.

The strains were acquired with six linear strain gauges located at the column mid length. One of the tests adopted a strain gauge at the centroid of each of the angle legs. The second test adopted two strain gauges at each angle leg as depicted in Figure 8. Figures 9 and 10 illustrates the test layout and the acquired stress *versus* strain curves.

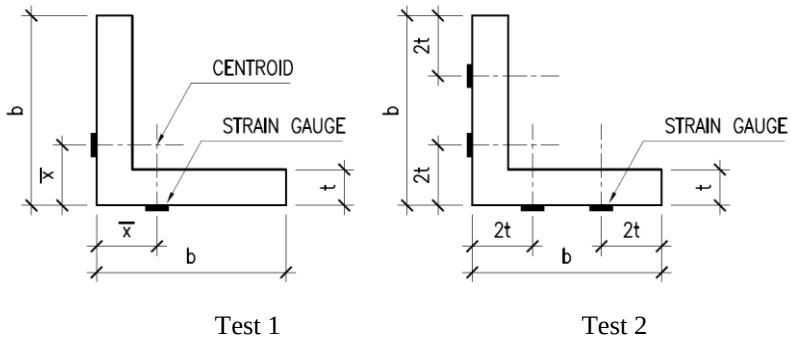


**Fig. 8 Material characterization tests adopted strain gauge layout**

**Fig. 9 Material characterisation test layout**

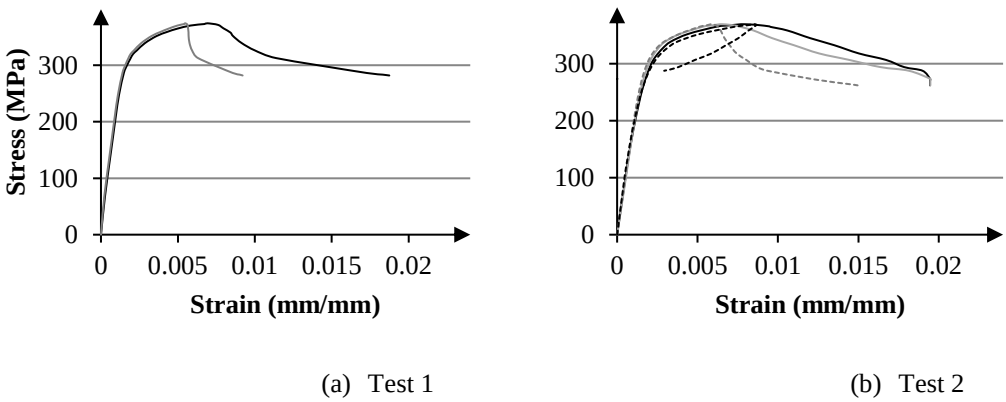


(a) Test 1 (b) Test 2

**Fig. 10 Material characterisation test stress *versus* strain curves**

Since the tests presented an ultimate load associated with a local buckling mode less than the typical tensile rupture load of coupon tests the values of the strains can not be considered valid after the ultimate test load (corresponding to a strain of 0.005). Figure 11 shows these results and the validity range of the experiments. Table 3 presents a summary of the tests regarding elasticity module, 0.2% stress, $\sigma_{0.2}$.

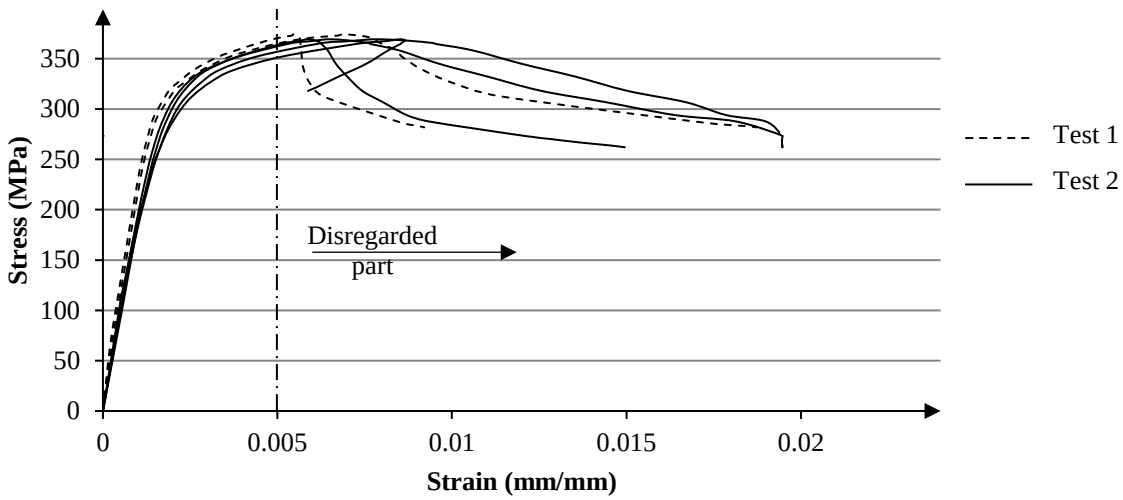


**Fig. 11 Final Material characterization test stress *versus* strain curves**

**Table 3 Summary of results of the characterisation tests**

| Test Specimen | E (GPa) | $\sigma_{0.2}$ (MPa) |
|---|---|---|

| | | |
|---|---|---|
| Test 1-S1 | 243.8 | 343 |
| Test 1-S2 | 219.4 | 352 |
| Test 2-S1 | 204.8 | 351 |
| Test 2-S2 | 189.2 | 335 |
| Test 2-S3 | 208.7 | 352 |
| Test 2-S4 | 200.5 | 353 |
| Average | 211.0 | 348 |

Additional analysis and the evaluation of the ultimate stress proposed by the CSM [2], $f_{csm}$ were made assuming a tensile rupture stress of 713 MPa obtained from tensile coupon test made on austenitic steels presenting a similar initial behaviour. The ultimate strain corresponding to this ultimate stress was equal to 45%.

## 3.4 Main tests instrumentation

The instrumentation used in the tests aimed to measure displacements through displacement transducers and deformations through rosettes strain gauges.

The LVDTs layout for monitoring the displacements varied for each test. Initially, for 1000 mm length columns, where a flexural buckling mode associated with a sinusoidal deformed shape were expected, the LVDTs were only located at the column mid length. This was confirmed in the tests, and since their ultimate loads indicated that the columns buckling coefficient "k" were less than 1.0, additional transducers were adopted, to acquire displacements along the column length.

After conducting the 1000 mm length tests, tests of 500 mm and 750 mm were performed where typical local buckling failures were expected. In these tests, the displacements at the column quarter points were helpful to compare them with the results at the column midpoint and enable a better depiction of the column deformed shape as the tests progressed.

Tests with1250 mm and 1500 mm were expected to fail by global flexural buckling and also adopted additional LVDTs at the column quarter height. Since the adopted hydraulic machine presented a hinge at the top, leading to possible rotations at this point, two LVDTs were used to evaluate these possible rotations. The adopted LVDTs layout can be visualised in Figure 12. Table 4 summarises the LVDTs configuration for each performed tests. Rosettes (Rectangular 45°) were adopted to acquire the strains and were positioned at the middle of the angles legs as can be observed in Figure 13.

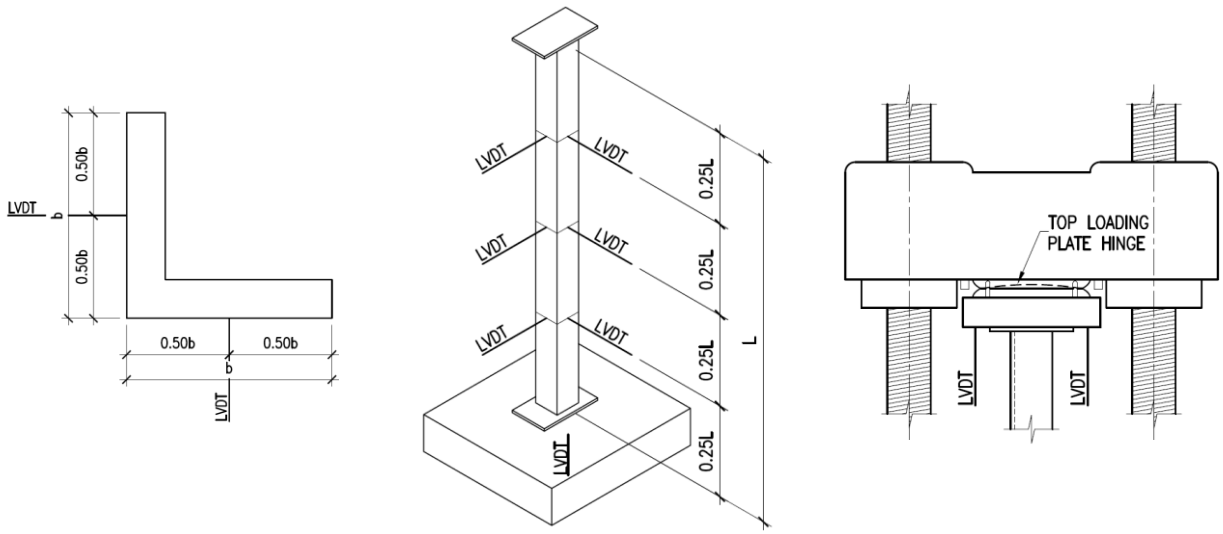


**Fig. 12 Tests adopted LVDTs layout along the column and the top loading plate**

**Table 4 Tests adopted LVDTs layout along the column and at the top and bottom loading plates**

| Test | LVDT's (25%L) | LVDT's (50%L) | LVDT's (75%L) | Bottom plate | Top plate |
|---|---|---|---|---|---|
| L64x64x6.4-AUS-500-1-23.09 | L | L | - | 2 | - |

| | | | | | |
|---|---|---|---|---|---|
| L64x64x6.4-AUS-500-2-23.09 | L | L | - | 2 | - |
| L64x64x6.4-AUS-750-1-27.09 | L | L | - | 2 | - |
| L64x64x6.4-AUS-750-2-28.09 | L | L | - | 2 | - |
| L64x64x6.4-AUS-1000-1-25.08 | - | L | - | 1 | - |
| L64x64x6.4-AUS-1000-2-01.09 | - | L | - | 2 | - |
| L64x64x6.4-AUS-1000-3-19.09 | L | L | - | 2 | - |
| L64x64x6.4-AUS-1250-1-05.10 | L | L | L | 2 | - |
| L64x64x6.4-AUS-1250-2-07.10 | L | L | L | 2 | L |
| L64x64x6.4-AUS-1500-1-13.10 | L | L | L | 2 | L |
| L64x64x6.4-AUS-1500-2-13.10 | L | L | L | 2 | L |

where,

L : actual measurement;

1 and 2 : number of LVDT's used at the bottom plate.

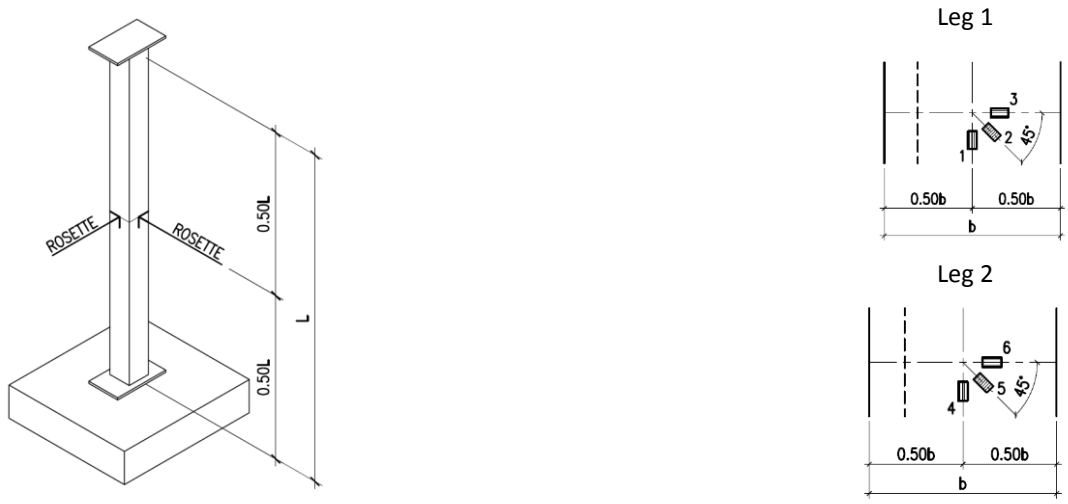


**Fig. 13 Tests strain-gauges layout**

## 3.5 Results

The tests presented a similar behaviour among the studied series. Figure 14 shows the load *versus* axial displacement curves for each column length tested. Table 5 summarises the ultimate loads obtained in the tests and their respective failure modes. The tests presented a local buckling of angle legs or a global flexural buckling. Flexural torsional buckling modes were not observed in the performed tests. Figures 15 and 16 illustrate the tests deformed configuration associated with failures related to local buckling and global flexural buckling.

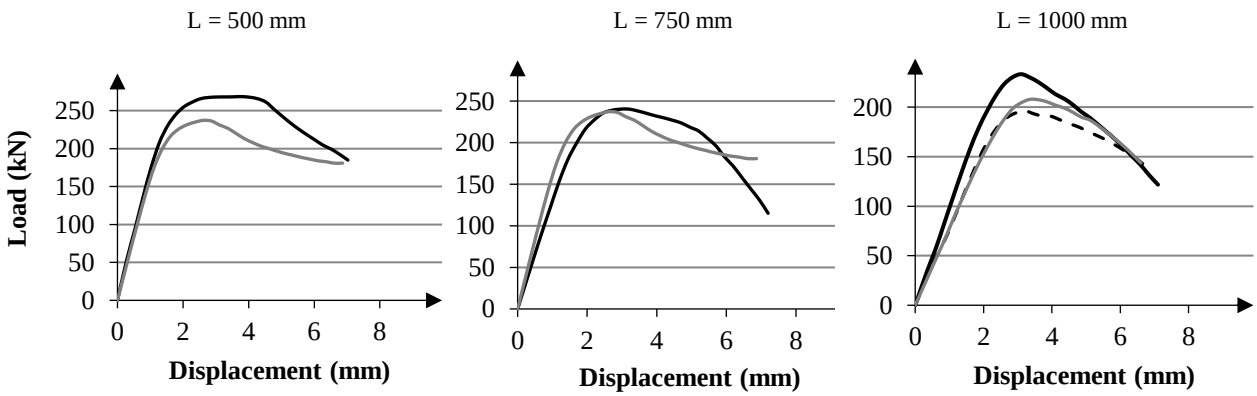

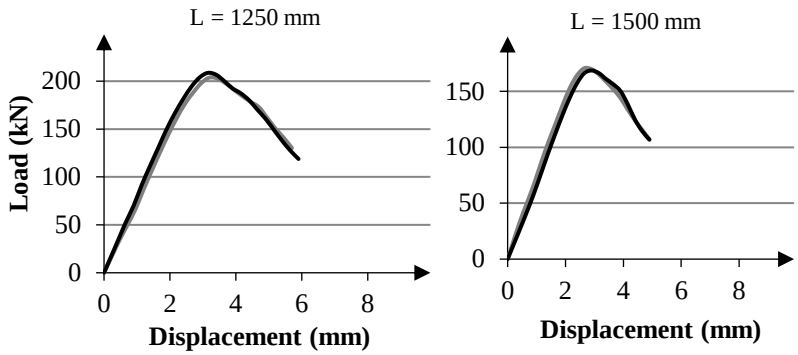


**Fig. 14 Tests load *versus* axial displacement curves**

**Table 5 Test results summary**

| Tests | Ultimate Load (kN) | Buckling Mode |
|---|---|---|
| Characterisation 1 | 283.6 | Local |
| Characterisation 2 | 287.4 | Local |
| L64x64x6.4-AUS-500-1-23.09 | 239.0 | Local |
| L64x64x6.4-AUS-500-2-23.09 | 272.4 | Local |
| L64x64x6.4-AUS-750-1-27.09 | 248.8 | Local |
| L64x64x6.4-AUS-750-2-28.09 | 241.7 | Local |
| L64x64x6.4-AUS-1000-1-25.08 | 209.7 | Flexural |
| L64x64x6.4-AUS-1000-2-01.09 | 197.3 | Flexural |
| L64x64x6.4-AUS-1000-3-19.09 | 234.8 | Flexural |
| L64x64x6.4-AUS-1250-1-05.10 | 205.4 | Flexural |
| L64x64x6.4-AUS-1250-2-07.10 | 212.1 | Flexural |
| L64x64x6.4-AUS-1500-1-13.10 | 172.8 | Flexural |
| L64x64x6.4-AUS-1500-2-13.10 | 170.9 | Flexural |

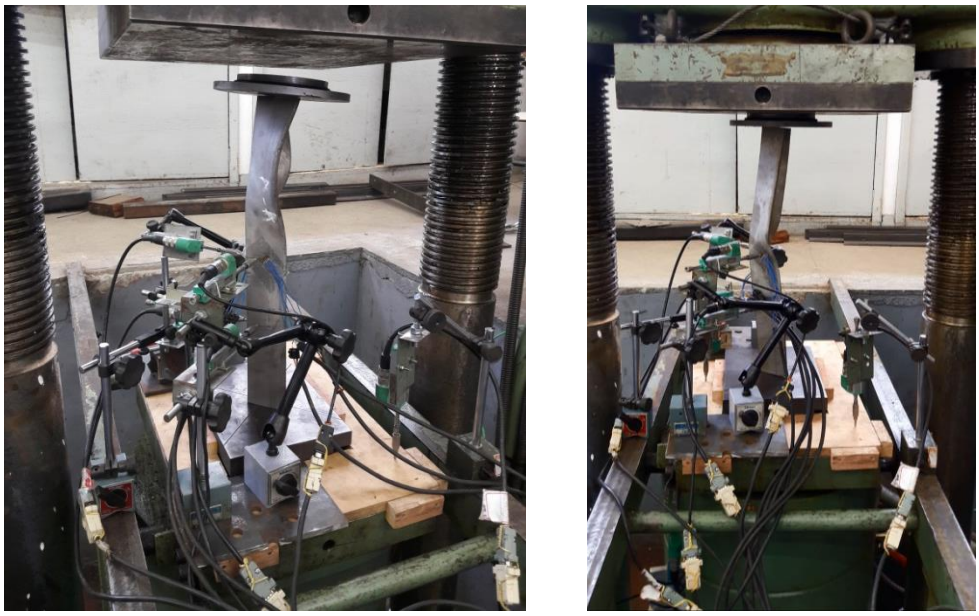

**Fig. 15 Deformed shape of 500mm columns associated with a local buckling failure**

**Fig. 16 Deformed shape of 1000mm columns associated with flexural buckling**

**Fig. 17 An overview of the deformed tested columns**

### 3.5.1 Rotation of the top loading plate

As mentioned before, in the 1250 mm and 1500 mm length column tests the possible rotations at the column top loading plate were acquired to confirm the columns support conditions throughout the experiments. Figure 18 shows the adopted LVDTs positioned for this purpose.

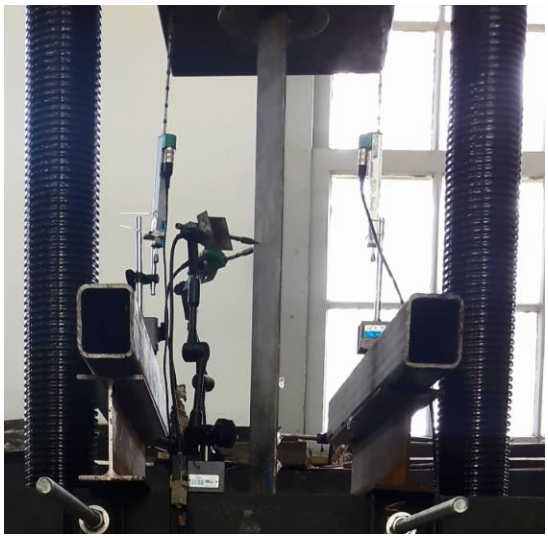

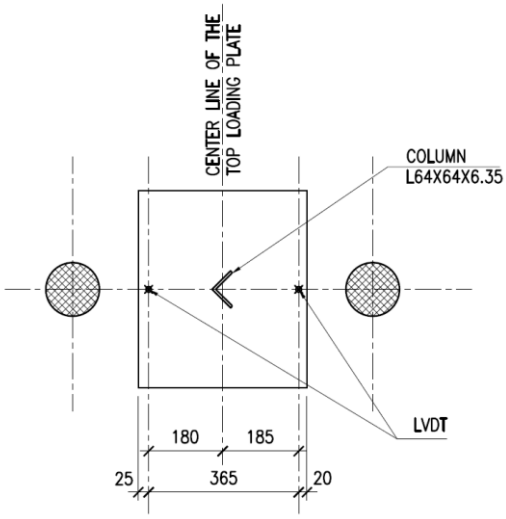


**Fig. 18 Layout of LVDTs utilised at the top loading plate**

Figure 19 shows the rotation at the column top loading plate evaluated with the already mentioned displacements transducers. The results confirmed that significant rotations only occurred after the columns ultimate load were reached.

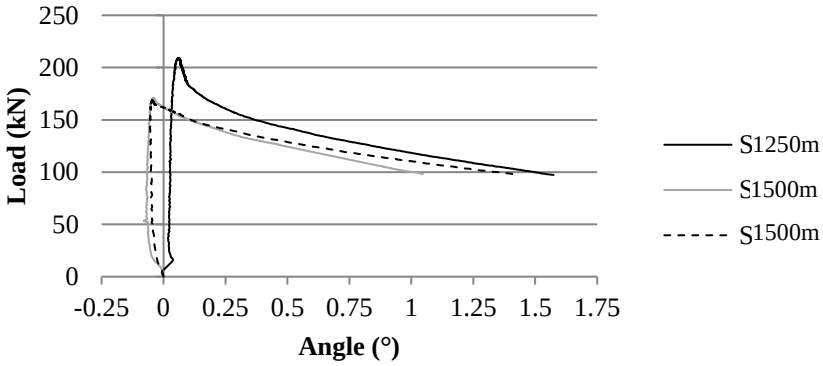


**Fig. 19 Top loading plate rotation**

## 4 Design Procedures Comparison

Table 6 summarises the tested columns ultimate loads evaluated using a buckling coefficient k = 0.5. In this table, the mean loads acquired in the tests appear in bold. In general, the Eurocode 3 Part 1-4 [1] proved to be conservative for the columns with a length less than or equal to 750 mm and unsafe for columns with a length greater or equal than 1250 mm. The CSM [2] proved to overestimate the ultimate loads of columns with a length greater or equal to than 500 mm.

**Table 6 Summary of test, design and critical loads**

| | | **L64x64x6,35** | | | | | |
|---|---|---|---|---|---|---|---|
| | | **Length (mm)** | | | | | |
| | | **250** | **500** | **750** | **1.000** | **1.250** | **1.500** |
| Load (kN) | Mean tests values | **285.5** | **255.7** | **245.3** | **213.9** | **208.8** | **171.9** |
| | $N_{Cr,u}$ | 62,102.3 | 15,525.6 | 6,900.3 | 3,881.4 | 2,484.1 | 1,725.1 |
| | $N_{Cr,v}$ | 15,911.3 | 3,977.8 | 1,767.9 | 994.5 | 636.5 | 442.0 |
| | $N_{Cr,T}$ | 653.1 | 653.1 | 653.1 | 653.1 | 653.1 | 653.1 |
| | $N_{Cr,FT}$ | 650.5 | 642.8 | 629.7 | 610.8 | 586.0 | 555.4 |
| | $N_{Cr,LB}$ | 618.7 | | | | | |
| | $N_{Rd,u}$ – EC3 | 319.2 | 308.0 | 297.6 | 287.6 | 277.7 | 267.7 |
| | $N_{Rd,v}$ – EC3 | 266.6 | 266.6 | 266.6 | 247.7 | 224.7 | **199.7** |
| | $N_{Rd,T}$ – EC3 | 217.8 | 217.8 | 217.8 | 217.8 | 217.8 | 217.8 |
| | $N_{Rd,FT}$ – EC3 | **217.7** | **217.1** | **216.2** | **214.7** | **212.7** | 210.0 |
| | $N_{Rd,u}$ – CSM | 423.30 | 406.40 | 390.70 | 375.40 | 360.00 | 344.20 |
| | $N_{Rd,v}$ – CSM | 406.80 | 376.20 | 345.50 | 311.70 | 274.00 | **234.50** |
| | $N_{Rd,T}$ – CSM | 270.90 | 270.90 | 270.90 | 270.90 | 270.90 | 270.90 |
| | $N_{Rd,FT}$ – CSM | **270.60** | **269.70** | **268.00** | **265.60** | **262.20** | 257.60 |
| | Eurocode 3 / Mean values | 0.76 | 0.85 | 0.88 | 1.00 | 1.02 | 1.16 |
| | CSM / Mean values | 0.95 | 1.05 | 1.09 | 1.24 | 1.26 | 1.36 |

Additionally, the failure modes predicted by the Eurocode 3 Part 1-4 [1] did not match the experimental failure modes, as can be seen in Table 7. At this point, it is fair to state that the α and $\lambda_0$ parameters adopted were not associated with rolled angle sections indicating the need for defining more accurate values for them. The theoretical buckling modes have also been determined being the smaller critical loads shown in Table 6.

For the investigated columns the stress predicted by the CSM [2], $f_{csm}$ was 464 MPa, i.e. 1.33 higher than the yield stress tension $f_y$ adopted by the Eurocode 3 part 1.4 [1]. The CSM [2] has been used without any restrictions beyond the ones established for the elements cross sections slenderness.

**Table 7 Comparison of buckling modes**

| | **L64x64x6.35** | | | | | |
|---|---|---|---|---|---|---|
| | **Length (mm)** | | | | | |
| | **250** | **500** | **750** | **1.000** | **1.250** | **1.500** |
| Theoretical | Local | Local | Local | Flexural | Flexural | Flexural |
| Tests | Local | Local | Local | Flexural | Flexural | Flexural |
| Eurocode 3 | Flexural Torsional | Flexural Torsional | Flexural Torsional | Flexural Torsional | Flexural Torsional | Flexural |

Figure 19 shows a comparison of the ratios of the ultimate column stress and the Austenitic steel yield stress acquired in the tests and the predictions made by Eurocode 3 Part 1-4 [1] and CSM [2]. The design prediction curves related to the Eurocode 3 Part 1-4 [1] and CSM [2] were determined according to the buckling phenomenon which controls the design related to the minor axis slenderness.

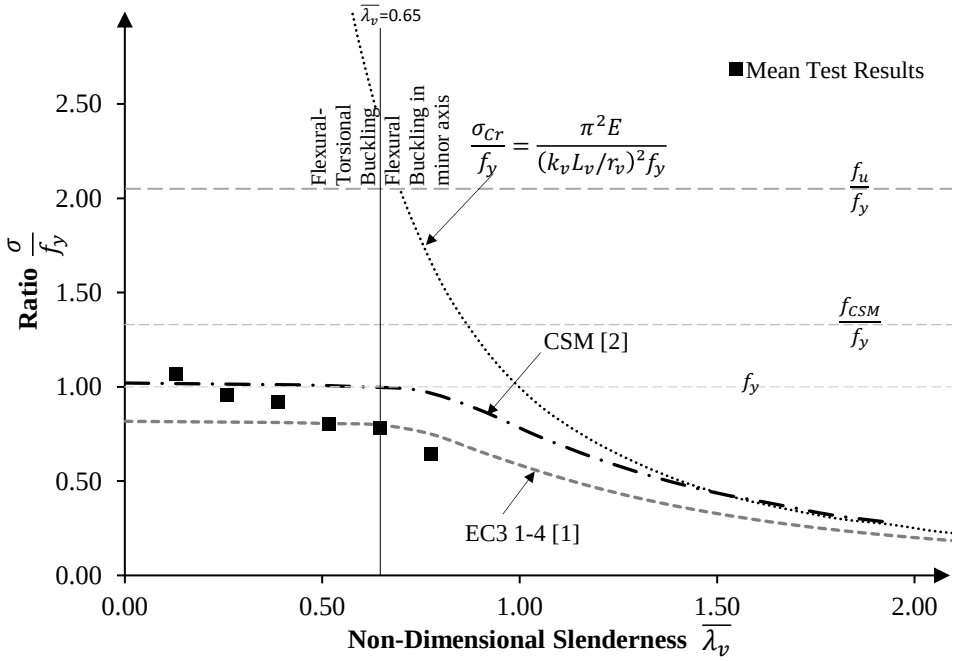


**Fig. 20 Final assessment of the tests results and design standards comparison**

## 5 Final Considerations

This paper presented an investigation of the structural behaviour of austenitic stainless steel angle columns. The thirteen experiments were made of austenitic stainless steel ASTM A276 304 in which two served for the material mechanical characterization. The columns tests were made of L64x64x6.35 sections with heights varying from 250 mm to 1500 mm. The test results were compared to the structural design criteria recommended by the Eurocode 3 Part 1-4 [1] and by the Continuous Strength Method - CSM [2].

The failure mode associated with the column tests were the local buckling of the angles legs for lengths less or equal than 750 mm and global flexural buckling for all others tested lengths. The flexural torsional buckling mode was not associated to any of the tested columns. The hinge located at the top of the adopted hydraulic machine did not interfere with the results up to the tests ultimate loads fact that was confirmed by LVTS used to acquire these rotations.

The test results indicated that for columns with normalised slenderness values less than 0.65, the Eurocode 3 Part 1.4 [1] design predictions led to conservative designs while for values above this normalised slenderness an overestimation of

the column load carrying capacity was reached. Additionally, the failure modes predicted by the Eurocode 3 Part 1.4 [1] did not match the experimental failure modes, as can be seen in Table 7. It is important to observe that the $\alpha$ and $\lambda_0$ parameters adopted were not associated with hot rolled angle sections indicating the need for defining more accurate values for them. The CSM [2] proved to overestimate the ultimate loads of columns with a length greater or equal to than 500 mm.

## References


[1] EUROCODE 3, EN 1993-1-4: 2006. Design of steel structures: Part 1-4: General rules – Supplementary rules for stainless steels. CEN, European Commit-tee for Standardization, Brussels.

[2] Ashraf, M., Gardner, L., 2013. The continuous strength method for structural stainless steel design. Thin-Walled Structures, vol. 68, p. 42–49.

[3] Baddoo, N.R., Burgan, B.A., Structural Design of Stainless Steel, SCI Publication P291, The Steel Construction Institute, Ascot, 2001